



Nanostructural analysis and textural modification of tilapia fish gelatin affected by gellan and calcium chloride addition



Li Cheng Sow^{a, b}, Yi Rui Peh^a, Bernadette Natalia Pekerti^a, Caili Fu^{a, c}, Nidhi Bansal^d, Hongshun Yang^{a, b, *}

^a Food Science and Technology Programme, c/o Department of Chemistry, National University of Singapore, Singapore 117543, Singapore

^b National University of Singapore (Suzhou) Research Institute, 377 Lin Quan Street, Suzhou Industrial Park, Suzhou, Jiangsu 215123, PR China

^c Fujian Putian Sea-100 Food Co., Ltd, Putian, Fujian 355000, PR China

^d School of Agriculture and Food Sciences, The University of Queensland, Brisbane 4072, Australia

ARTICLE INFO

Article history:

Received 16 January 2017

Received in revised form

9 July 2017

Accepted 10 July 2017

Available online 11 July 2017

Keywords:

Fish gelatin

Gellan

Calcium chloride

Fourier transform infrared spectroscopy

(FTIR)

Atomic force microscopy (AFM)

ABSTRACT

Fish gelatin (FG) is more suitable for consumption by religious people than mammalian gelatin. One common modification method of FG is mixing FG with polysaccharides. However, the mechanism is not clear. We found that FG gel containing 0.1 g/100 mL gellan, 20 mmol/L CaCl₂ and 6.67 g/100 mL FG (180 Bloom) matched gel strength, hardness, cohesiveness, chewiness as well as gelling temperature (T_g) and melting temperature (T_m) of commercial beef gelatin (BG) (240 Bloom). The modified FG was also observed by the result of helix/coil ratio and spherical aggregates. The modification decreased the diameter of FG's aggregates from 472 to 249 nm, which matched with BG (272 nm, $P < 0.05$). Co-existence of segregative gellan-gellan fibrous aggregates and associated FG-gellan amorphous structure were also identified at the modified FG by atomic force microscope (AFM). The helix/coil ratio and diameter of spherical aggregates were inversely correlated, the mechanism behind was the strength of gelatin association. The involvement of hydrogen bond and presence of FG-gellan complex have been validated by urea addition and Fourier transform infrared (FTIR) spectroscopy. A schematic model was proposed. As modified FG successfully matched the of texture properties of BG, it is promising to replace BG with FG.

© 2017 Elsevier Ltd. All rights reserved.

1. Introduction

Gelatin is a multifunctional ingredient that has growing demand in food and pharmaceutical industry. Commonly extracted from pork skin or beef bone (Ahmad & Benjakul, 2011), often mammalian gelatin is not suitable for religious people who account for about 45.5% of world population and can't consume pork or beef products (Pew Research Center, 2014). Fish gelatin (FG) is one of the alternative replacers of mammalian gelatin. By utilising fishery by-products such as FG, economic and environmental burden could be reduced as well (Feng, Fu, & Yang, 2017).

However, FG has lower gel strength, gelling temperature (T_g) and melting temperature (T_m) than mammalian gelatin (Kaewruang, Benjakul, Prodpran, Encarnacion, & Nalinanon, 2014).

FG could be modified to improve the physicochemical properties, and one of the common and promising methods is through mixing FG with other polysaccharides (Derkach, Ilyin, Maklakova, Kulichikhin, & Malkin, 2015). For example, the addition of gellan and carrageenan improved the mechanical strength, T_m and T_g of tilapia FG film (Pranoto, Lee, & Park, 2007). Type B bovine gelatin mixed with κ -carrageenan resulted in faster gelation, higher yield stress and lower deformation strain than gelatin alone (Derkach et al., 2015). Panouillé and Larreta-Garde (2009) reported that mixed gel containing calcium, alginate and type A porcine gelatin had higher shear modulus and lower $\tan \delta$ than alginate or gelatin gels. Lau, Tang, and Paulson (2000, 2001) who conducted comprehensive studies of mixed gel (1.6 g/100 g total solid) containing gellan and type B bovine gelatin. They found that increasing gellan to gelatin ratio increased the hardness and gelation rate. In addition, the maximum hardness, brittleness, cohesiveness and gelation rate were achieved the optimum level of calcium ions were added (Lau et al., 2000, 2001). It was also found that NaCl could

* Corresponding author. Food Science and Technology Programme, c/o Department of Chemistry, National University of Singapore, Singapore 117543, Singapore.
E-mail address: chmyngs@nus.edu.sg (H. Yang).

modify physicochemical properties of the gellan and type A porcine gelatin gel (1 g/100 g total solid) (Lee et al., 2003).

The use of mixed biopolymer system is important and common in food industry because the final physicochemical properties of the mixed biopolymer system could be customised and finely controlled (Yasin, Babji, & Ismail, 2016). Mixing of biopolymers often result in phase separation due to associative or segregative interaction, and the event of gelation adds complexity to the structure (Panouillé & Larreta-Garde, 2009). Although mixing of gellan into gelatin has been studied in the form of gel (Lau, Tang, & Paulson, 2001, 2000; Lee et al., 2003) and film (Pranoto et al., 2007), the impact of gellan mixing with tilapia fish gelatin, especially the effect at the secondary structural and nanostructure level, as well as possibility of using gellan-FG as mammalian gelatin replacer remain to be explored.

The current study therefore aims to use gellan and calcium chloride to modify the texture of FG gel with reference to beef gelatin (BG), as textural properties of food are the determining factors on product quality and consumer acceptance. The T_m and T_g of the modified gelatin gels were investigated by rheological measurements. The secondary structure and nanostructure were examined by AFM and FTIR spectroscopy. The study furthers the understanding of the relationship between structure and physicochemical properties in FG modification.

2. Materials and methods

2.1. Materials

Tilapia skin FG (160 Bloom) and BG (240 Bloom) were from Jiangxi Cosen Biology Co., Ltd (Jiangxi, China) and Jingrong co., Ltd (Fujian, China), respectively. Deacetylated gellan (Kelcogel, 77109A) was sponsored by CP Kelco (Atlanta, GA, USA). Calcium chloride dihydrate ($\text{CaCl}_2 \cdot 2\text{H}_2\text{O}$) was from Merck (Billerica, MA, USA).

2.2. Sample preparation

Gelatin gel was prepared following the method of Sow and Yang (2015). Briefly, gelatin solution was heated and swirled in 65 °C water bath for 10 min. Gellan solution was heated and stirred at 95 °C until dissolved and combined with FG solution at 1:1 (mL: mL). In all formulations, the final concentration of gelatin in the mixture was 6.67 g/100 mL and the final concentration of gellan ranged from 0.05 to 0.5 g/100 mL. For CaCl_2 , the final concentration was from 0.5 to 30 mmol/L. All samples were transferred in cylindrical containers and stored at 10 ± 2 °C refrigerator for 17 ± 1 h before texture measurement.

2.3. Gel strength and texture profile analysis (TPA)

After storage at 10 °C for 17 ± 1 h, the gel was removed from containers and measured the gel strength and TPA by a TA.XT2-i Texture Analyser (Stable Micro System, Surrey, UK) according to the procedure described by Sow and Yang (2015).

2.4. T_m and T_g

The gel samples of 2.5 cm diameter and 0.8 cm thickness were placed on an Anton Paar MCR-102 (Anton Paar, OR, USA) stress-controlled rheometer equipped with a stainless steel 25-mm-diameter parallel plate geometry. Linear viscoelastic region was pre-determined by performing stress (0.1–100 Pa) and frequency sweep (0.1–100 Hz) at 10 °C. Temperature sweep from 10 °C to 40 °C (for T_m), followed by 40 °C–10 °C (for T_g) at a scan rate of 1 °C/min, frequency of 1 Hz and stress of 5 Pa was carried out. T_m and T_g

were calculated as temperature when cross-over of elastic modulus (G') and loss modulus (G'') occurred (Boran, Mulvaney, & Regenstein, 2010).

2.5. Atomic force microscopy (AFM)

The nanostructure of gelatin was characterised by TT-AFM (AFM workshop, Signal Hill, CA, USA) following procedures described previously (Yang & Wang, 2009; Feng, Bansal, & Yang, 2016; Feng, Ng, Miks-Krajnik, & Yang, 2017). Gelatin solution was diluted 20 times and pipetted onto a freshly cleaved mica sheet. The AFM was equipped with AppNano ACLA-10 probe (Applied NanoStructures, Mountain View, CA, USA) with resonance frequency of 160–225 kHz and force constant of 36–90 N/m. The quantitative analysis of AFM was performed using Gwyddion software (<http://gwyddion.net>).

2.6. Turbidity

Turbidity and zeta potential were measured according to Razzak, Kim, and Chung (2016) with some modification. For turbidity, the solutions (as in section 2.2) were incubated for 1 h at 10 °C, the absorbance at 600 nm was recorded using UV-VIS spectrophotometer (Shimadzu Corporation, Kyoto, Japan). The turbidity was defined as

$$\tau = -\frac{1}{L} \ln\left(\frac{I}{I_0}\right), \quad (1)$$

where I is the intensity of radiation transmitted through the mixture, I_0 is the incident radiation intensity, L is the path length of the light.

2.7. Fourier transform infrared spectroscopy (FTIR)

Spectrum One FTIR spectrometer (PerkinElmer, Waltham, MA, USA) was employed to characterise the secondary structure of lyophilised gelatin according to Sow and Yang (2015). All the spectra were pre-processed (baseline corrected, smoothed and normalised) using Spectrum software (version 5.0.5, PerkinElmer), followed by deconvoluted (gamma: 1.5, smoothing: 50%–60%), Gaussian curve fitting of deconvoluted amide I ($1600 - 1700 \text{ cm}^{-1}$) was performed using Origin Pro 9 (OriginLab, Northampton, MA, USA). The fitting quality of the Gaussian curves was confirmed by having $R^2 > 0.992$.

2.8. Statistical analysis

At least three samples were prepared for each experiment, and the experiment was conducted in triplicate. All the results were reported as mean \pm standard deviation and subject to ANOVA and Tukey HSD's multiple range test using IBM SPSS Statistics for Windows, version 20.0 (IBM, Chicago, IL, USA) to determine the statistical difference.

3. Results and discussion

3.1. Gel strength, TPA, T_m and T_g

Gellan ranging from 0.05 to 0.5 g/100 mL was added into FG (Fig. 1). When the concentration of gellan increased, the gel strength, hardness and chewiness of FG increased while cohesiveness and springiness decreased. The ability of gellan to improve the properties of FG was consistent to previous reports (Fonkwe, Narsimhan, & Cha, 2003; Lau et al., 2000; Lee et al., 2003;

Pranoto et al., 2007), possibly due to the ability of gellan and gelatin to form “heterolytic junction zones” (Fonkwe et al., 2003). Gel strength is an important quality indicator of gelatin that determines its commercial value (Sow & Yang, 2015). When compared to the target BG, 0.1 g/100 mL of gellan was sufficient to increase the gel strength and hardness of FG to the level of BG (Fig. 1a–b), although the springiness and cohesiveness were still lower than that of BG (Fig. 1c–d).

The properties of FG and gellan being sensitive to salts were employed to further modify the texture of FG–gellan gel. CaCl₂ was added to the mixture of FG and 0.1 g/100 mL gellan (FGe) and the impact was shown in Table 1. Addition of CaCl₂ up to 5 mmol/L increased the gel strength of FGe to a level even higher than BG (317.6 vs. 212.6 g); however, above 20 mmol/L of CaCl₂, the gel strength decreased. When CaCl₂ was increased from 0.5 to 15 mmol/L, the cohesiveness of FGe decreased. The cohesiveness was increased to maximum at 20 mM CaCl₂. The current sensitivity of gellan to CaCl₂ concentration agreed with the result of Lau et al. (2000). Ca²⁺ can directly bind to the anionic domain (COO⁻) of

gellan to crosslink the polysaccharide chains, thus when the crosslinking is optimum, maximum gel strength could be achieved (Morris, Nishinari, & Rinaudo, 2012). Above optimum Ca²⁺ concentration, excessive gellan association and large aggregates affected the junction zones formation and decreased the gel strength (Morris et al., 2012).

Table 2 shows the T_m and T_g of the control FG and BG, FGe gel with 5 mmol/L CaCl₂ (FGe5C) and 20 mmol/L (FGe20C). Addition of 0.1 g/100 mL gellan increased T_m of FG. Increasing CaCl₂ concentration, the T_g of the modified FG gels increased. Overall, T_m and T_g of FGe20C has no statistically significant difference (*P* > 0.05) with BG.

3.2. Nanostructure by AFM

To elucidate the structure modification caused by gellan and CaCl₂ addition, AFM was employed to characterise FG, BG, FGe, FGe5C and FGe20C. The FGe samples with 5 mmol/L (FGe5C) and 20 mmol/L (FGe20C) CaCl₂ were selected as the representative

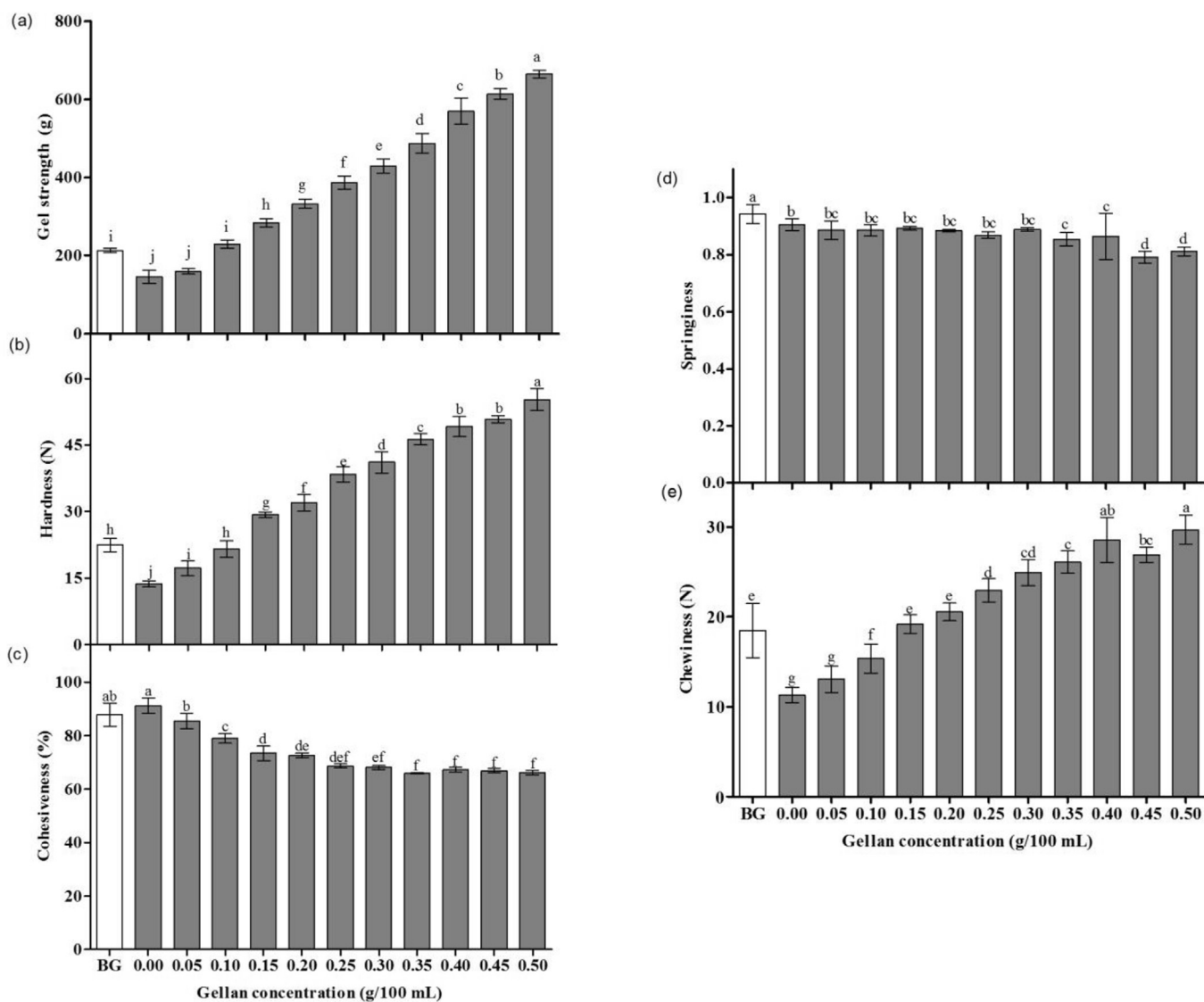


Fig. 1. Effects of gellan concentration on (a) gel strength, (b) hardness, (c) cohesiveness, (d) springiness, (e) chewiness of 6.67 g/100 mL fish gelatin (FG, ■) with reference to beef gelatin (BG, □).

*Means with different lowercase letters are significantly different (*P* < 0.05) among different groups.

Table 1
Effects of CaCl₂ addition on the TPA and gel strength of fish gelatin (FG) and 0.1 g/100 mL gellan-FG mixed gel. *Within each column, means with different lowercase letters are significantly different ($P < 0.05$) among different groups.

Gel	[CaCl ₂](mmol/L)	Gel strength (g)	Hardness (N)	Springiness	Cohesiveness (%)	Chewiness (N)
Beef gelatin	0	212.6 ± 5.4 ^{de}	22.46 ± 1.53 ^{cd}	0.943 ± 0.033 ^a	87.81 ± 4.35 ^b	18.45 ± 3.01 ^{abc}
Fish gelatin	0	144.8 ± 16.7 ^f	13.72 ± 0.55 ^f	0.906 ± 0.017 ^{bc}	91.37 ± 2.45 ^a	11.37 ± 0.73 ^f
Fish gelatin +0.1 g/100 mL Gellan	0	228.3 ± 9.2 ^{cd}	21.10 ± 1.70 ^{de}	0.888 ± 0.018 ^{bc}	80.40 ± 2.65 ^{de}	15.25 ± 1.32 ^{de}
	0.5	244.0 ± 2.0 ^c	20.16 ± 0.23 ^e	0.878 ± 0.013 ^c	83.54 ± 1.94 ^{cd}	14.79 ± 0.64 ^e
	1.25	279.0 ± 4.5 ^b	23.09 ± 0.44 ^{bcd}	0.894 ± 0.006 ^{bc}	80.78 ± 0.87 ^{de}	16.68 ± 0.42 ^{cdef}
	2.5	302.3 ± 4.3 ^{ab}	25.07 ± 0.61 ^b	0.891 ± 0.019 ^{bc}	79.87 ± 0.49 ^e	17.84 ± 0.71 ^{abcd}
	5	317.6 ± 26.2 ^a	28.94 ± 1.22 ^a	0.894 ± 0.021 ^{bc}	72.89 ± 2.76 ^g	18.86 ± 0.93 ^{ab}
	10	315.3 ± 5.8 ^a	29.84 ± 1.23 ^a	0.892 ± 0.013 ^{bc}	72.24 ± 1.53 ^g	19.21 ± 0.74 ^a
	15	285.4 ± 5.7 ^b	27.99 ± 1.25 ^a	0.913 ± 0.026 ^{ab}	75.11 ± 1.09 ^{fg}	19.21 ± 1.28 ^a
	20	209.7 ± 21.2 ^{de}	22.55 ± 0.95 ^{cd}	0.905 ± 0.012 ^{bc}	85.75 ± 1.02 ^{bc}	17.58 ± 0.71 ^{abcd}
	25	212.1 ± 19.6 ^{de}	23.84 ± 1.93 ^{bc}	0.909 ± 0.012 ^b	78.13 ± 0.72 ^{ef}	16.94 ± 1.51 ^{bcd}
	30	197.5 ± 17.2 ^e	22.19 ± 1.86 ^{cde}	0.897 ± 0.024 ^{bc}	78.86 ± 1.02 ^e	15.71 ± 1.54 ^{def}

Table 2
Summary of nanostructures present in different gelatin gels (Absence (X)/presence (√)) and the results of gel-sol-gel transition. *Within each row, means with different lowercase letters are significantly different ($P < 0.05$) among different groups.

	BG	FG	FGe	FGe5C	FGe20C
Spherical aggregates	√	√	√	√	√
Diameter (nm)	272 ± 158 ^{bc}	472 ± 258 ^a	323 ± 192 ^b	286 ± 114 ^{bc}	249 ± 109 ^c
Height (nm)	8.9 ± 11.8 ^d	12.7 ± 12.4 ^{cd}	44.2 ± 39.2 ^a	15.9 ± 11.5 ^{bc}	19.7 ± 21.7 ^b
Irregular aggregates	√	√	√	√	√
Cavity	√	√	X	√	√
Fibril strands	X	X	√	√	√
Rod-like structure	√	√	X	X	X
Amorphous structure	X	X	√	X	√
Fibrous aggregate	X	X	X	√	√
Ring-like structure	√	√	X	X	√
T _m (°C)	32.1 ± 0.3 ^a	28.0 ± 0.6 ^d	30.2 ± 0.6 ^{bc}	29.6 ± 0.1 ^c	30.9 ± 0.4 ^{ab}
T _g (°C)	28.5 ± 1.8 ^a	21.7 ± 0.6 ^b	21.9 ± 0.7 ^b	23.3 ± 0.7 ^b	25.9 ± 4.1 ^{ab}

samples, as FGe5C shows maximum gel rigidity (FGe5C) and FGe20C shows the optimum gel texture close to BG.

The state of aggregation of gelatin molecules is related to the macroscale properties (Liu & Wang, 2011). Table 2 summarises the heterogeneous structure of gelatin identified. Spherical aggregates and irregular aggregates, common features for low concentration gelatin, were observed in all the samples (Yang & Wang, 2009). Interestingly, FG modified with gellan and CaCl₂ showed new structures including fibril strands, amorphous structure and fibril aggregates (Fig. 2). The representative nanostructure of FGe was the amorphous structure (Fig. 2e–f), while the segregated fibril and spherical aggregates was dominant in FGe5C (Fig. 2g–h). FGe20C represented the heterogeneity with mixture of fibril strands, fibrous aggregates, amorphous structure and spherical aggregates (Fig. 2i–j).

The presence of amorphous structure might represent the associative complexation of FG and gellan that appeared as one phase (Hans Tromp, van de Velde, van Riel, & Paques, 2001). Fibril strands were the representative structure of gellan (Funami et al., 2008), which can aggregate to form fibrous aggregates such as those observed in FGe5C & FGe20C. As a comparison, fibrous aggregates of gellan were not identified in FGe due to the absence of Ca²⁺ to crosslink gellan. Addition of CaCl₂ firstly induced crosslinking and gelation of gellan, as the temperature decreased to the gelling point of FG, FG further gelled within the gellan network as a bi-continuous network, a typical structure due to segregative interaction (Funami et al., 2008; Hans Tromp et al., 2001). This phenomenon was also reported by Pang, Deeth, Sopade, Sharma, and Bansal (2014) that in milk protein-gelatin system, casein micelles were segregated from gelatin, which was correlated with enhanced viscoelastic properties of the mixed-gel.

The dominant of fibrous aggregates in FGe5C indicated that 5 mM CaCl₂ crosslinked gellan intensively, which induced segregative interaction between FG and gellan, hence FG-FG association that appeared as individual spherical aggregates. Segregative interaction of FG and gellan was likely weakened in FGe20C, as the frequency of fibrous aggregates being observed reduced, and the fibril strand (non-crosslinked gellan) and amorphous structure (FG-gellan complex) re-appeared. This is due to excessive Ca²⁺ that occupied the charged side of gellan chains, hence reduced the crosslinked gellan-gellan strands (Lee et al., 2003), as a result, FG re-associated with free gellan strands.

Quantitative analysis of the height and diameter of spherical aggregates were performed (Table 2 and Fig. S1). The averaged diameter and height of BG were smaller than those of FG, respectively. The large aggregates of FG compared to BG could be due to the difference in molecular weight (MW) and the gelatin-gelatin aggregation (Saxena, Sachin, Bohidar, & Verma, 2005). High MW gelatin (protein) tends to aggregate more than low MW gelatin (Saxena et al., 2005). Moreover, the presence of high MW fractions in FG might result in poorer physicochemical properties as compared to porcine and bovine gelatin (Mohtar, Perera, & Quek, 2010). It was observed that the larger the spherical aggregates, the poorer the textural properties of FG compared to BG. Similarly, it was reported that increased spherical aggregates size due to NaCl addition resulted in a weaker FG gel (Sow & Yang, 2015).

Table 2 shows the averaged diameter of FG was greater than that of all the modified FG. The reason might be that gellan and CaCl₂ might compete the water of hydration and reduce the swelling of FG. Moreover, in FGe5C and FGe20C segregative interaction occurred, thus FG-FG associated stronger, resulting in even smaller diameter of spherical aggregates. The spherical aggregates of FGe5C

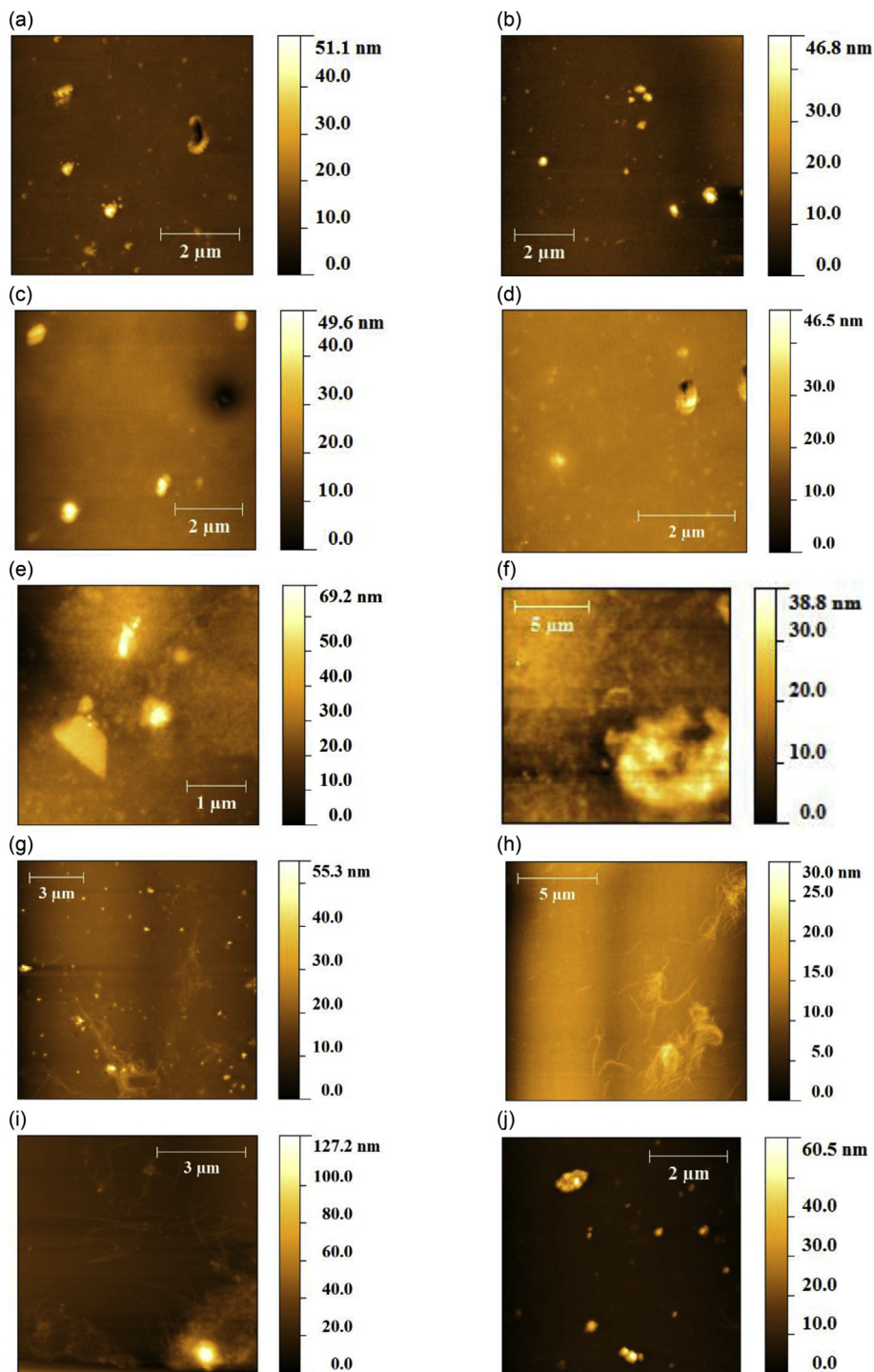


Fig. 2. Nanostructure morphologies of (a, b) beef gelatin (BG); (c, d) fish gelatin (FG); (e, f) fish gelatin with 0.1 g/100 mL gellan (FGe); (g, h) fish gelatin with 0.1 g/100 mL gellan and 5 mmol/L CaCl_2 (FGe5C); (i, j) fish gelatin with 0.1 g/100 mL gellan and 20 mmol/L CaCl_2 (FGe20C) imaged by AFM.

and FGe20C similar to that of BG, supporting the significant relationship between aggregate size and textural properties. For the average height of spherical aggregates, in FGe it increased significantly due to the presence of aggregates with height greater than 50 nm (Fig. S1), which might indicate the presence of FG-gellan coacervates. As gellan-gellan crosslinks increased, FG-gellan coacervates decreased, thus the average height of the spherical aggregates in FGe5C and FGe20C decreased compared to FGe.

3.3. Schematic model

A schematic model was proposed to demonstrate the texture and structure modification of FG by gellan and CaCl_2 (Fig. 3). The various nanostructures, mainly spherical aggregates, fibril strands and fibrous aggregates and the amorphous structure were shown due to the results of gelatin-gelatin, gelatin-gellan or gellan-gellan interaction. The type and magnitude of interactions affected the

macro 3-D structure and hence physicochemical properties.

Spherical aggregates' diameter was one of the determining factors of gelatin texture. The dimension of spherical aggregates was proposed related to the association of gelatin chains, as such stronger association among gelatin chains resulted in a more compact and rigid structure with smaller nanosphere' dimension as in BG and FGe20C. In contrast, FG possessed large nano-spherical aggregates. Extrapolating the nanoscale observation to macro-observation, this led to a coarser packing and less rigid 3D gel with compromised gel strength and hardness.

The associative complex formed by FG and gellan represented as amorphous structure in AFM. The proposed model illustrated the H-bond formation between NH group from gelatin and COO⁻/OH group of gellan as one of the possible forces contributing to the associative complexation (Fig. 3). The amorphous structure could improve the hardness and gel strength of the FG, as proven from the result of FGe in Fig. 1 & Table 1, although cohesiveness of the gel was different from the reference BG.

The fibrous aggregates were identified as Ca²⁺ crosslinked gellan which was dominant in FGe5C. However, the gel formed by the intensive crosslinked gellan in FGe5C was too hard and not cohesive (Table 1), thus rendered the texture of FGe5C undesirable as BG replacer. On the other hand, the crosslink gellan-gellan was reduced at excess CaCl₂ (FGe20C), the non-crosslinked gellan therefore interacted with gelatin to restore amorphous structure. The co-existence of partially crosslinked gellan, spherical aggregates and amorphous structure in FGe20C is critical to match the textural properties of BG. The gel strength and hardness of the FGe20C network were supported by amorphous structure, partially crosslinked fibrous aggregates of gellan, as well as the small and compact FG spherical aggregates (similar dimension to BG). As for

the significant increase in the cohesiveness of FGe20C, it could be explained by the decreased amorphous structure and fibrous aggregates that contributed to low cohesiveness when compared to FGe and FGe5C, respectively. This is supported by the report of Nieto Nieto, Wang, Ozimek, and Chen (2016) which concluded that the balance between repulsive and attractive forces is important for the properties of protein-polysaccharide gel. The key to a successful modification thus relied on balance of gellan-gellan and gellan-gelatin interaction, also both fibrous aggregates and amorphous structure need to be present to make modified FG suitable replacer of BG.

3.4. Schematic model validation

3.4.1. Turbidity and gel strength

Turbidity and gel strength (Table 3), and their changes due to the addition of urea (1 mol/L) were evaluated. The increased in turbidity of FGe confirmed the presence of associative complexes between FG and gellan (Nieto Nieto et al., 2016). In FGe5C, the turbidity increased to maximum possibly due to the increased association of gellan-gellan aggregates and FG-FG chain. In FGe20C, as the gellan was not intensively crosslinked as in FGe5C, the turbidity hence decreased to the level of FGe.

Urea (1 mol/L) as H-bond breaker (Nieto Nieto et al., 2016) was added to identify the role of H-bond in FG-FG and FG-gellan interaction. The turbidity of all samples was decreased upon urea addition. The ability of urea to decrease the turbidity of FGe to the level of FG confirmed the presence of H-bond in FG-gellan complexation. Because urea was unable to disrupt crosslinked gellan, the turbidity of CaCl₂-added mixtures was still higher than FG and FGe after urea addition.

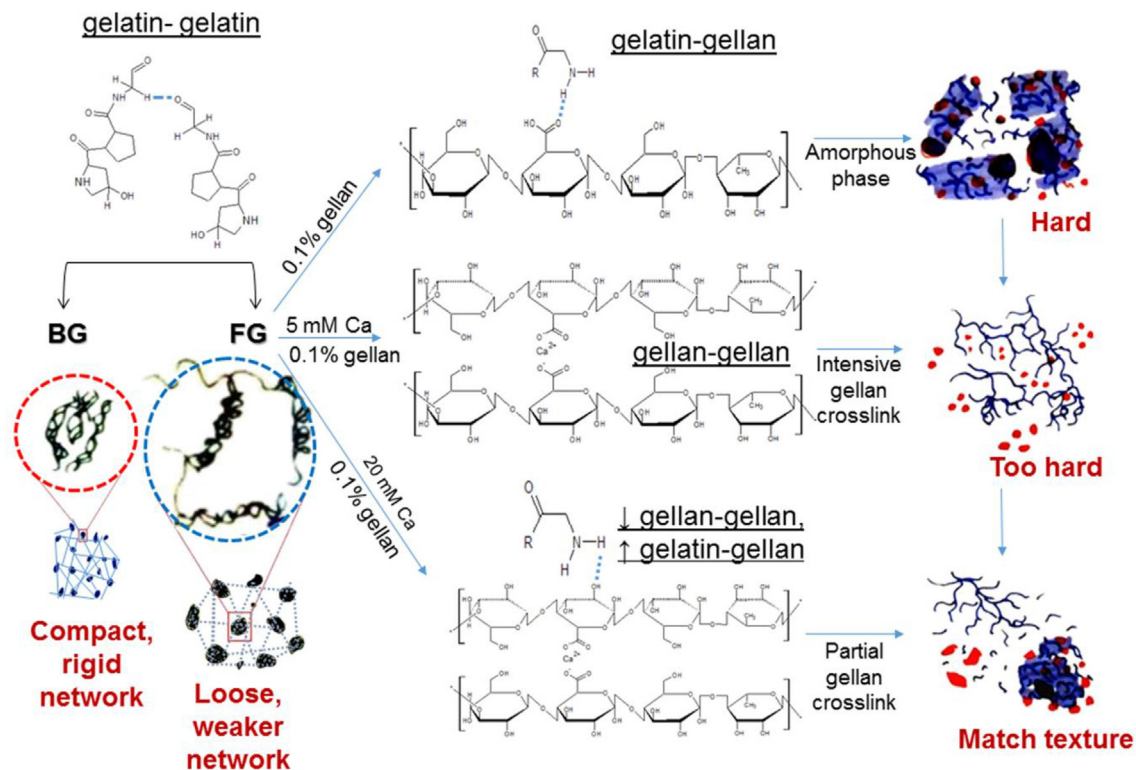


Fig. 3. Schematic model illustrating the modification of fish gelatin (FG).

*Red spherical aggregates (■) represented gelatin; blue fibril strands (■) represented gellan; dark blue large spherical aggregates (■) indicated the coacervates of both biopolymers. *Chemical structures not presented according to actual ratio, for illustration purpose only. (For interpretation of the references to colour in this figure legend, the reader is referred to the web version of this article.)

Table 3

Effect of urea (1 mol/L) on turbidity and gel strength of fish gelatin (FG) and modified FG samples. *Within each column, means with different lowercase letters are significantly different ($P < 0.05$) among different groups. Within each parameter, means with different uppercase letters are significantly different.

Sample	Turbidity (cm^{-1})		Gel strength (g)	
	Control	1 mol/L urea	Control	1 mol/L urea
FG	$0.55 \pm 0.05^{\text{Ac}}$	$0.41 \pm 0.02^{\text{Bb}}$	$144.8 \pm 16.7^{\text{Ac}}$	$81.9 \pm 1.8^{\text{Bc}}$
FGe	$0.62 \pm 0.02^{\text{Ab}}$	$0.44 \pm 0.03^{\text{Bb}}$	$228.3 \pm 9.2^{\text{Ab}}$	$96.6 \pm 1.0^{\text{Bb}}$
FGe5C	$0.8 \pm 0.02^{\text{Aa}}$	$0.56 \pm 0.12^{\text{Ba}}$	$317.6 \pm 26.2^{\text{Aa}}$	$153.1 \pm 4.3^{\text{Ba}}$
FGe20C	$0.65 \pm 0.02^{\text{Ab}}$	$0.52 \pm 0.07^{\text{Ba}}$	$209.7 \pm 21.2^{\text{Ab}}$	$149.9 \pm 3.5^{\text{Ba}}$

The gel strength also responded to urea addition. For FG treated with urea, the gel strength reduced due to the disruption of H-bond. The FG-gellan complex stabilised by H-bond was also disrupted by urea addition, as such the reduction of gel strength in FGe was even more than that of FG. As a comparison, the gel strength of FGe5C and FGe20C remained higher than that of FGe with urea addition, as the calcium crosslinked gellan was not sensitive to urea.

3.4.2. FTIR

FTIR spectra of the FG, BG and modified FG were collected (Fig. S2) to validate the proposed schematic model from the aspect of interaction between the functional groups and the secondary structure of protein.

The characteristic bands and peaks including amide A, amide B, amide I, amide II and amide III were identified and shown in Table 4. Amide A peak represents the stretching of N-H bond (Ahmad & Benjakul, 2011), the wavenumber of amide A peak of FG and BG showed that the N-H group was in free NH stretching vibration ($3400\text{--}3440 \text{ cm}^{-1}$) (Singh, Benjakul, Maqsood, & Kishimura, 2011). Hydrogen bonding at N-H site resulted in elongation of the N-H bond (Myshakina, Ahmed, & Asher, 2008). As a consequence, the amide A peak was down-shifted as observed in gellan and CaCl_2 modified FG. H-bond could be formed between the NH residue and C=O group from gelatin's peptide chains (gelatin-gelatin H-bond) (Singh et al., 2011). Moreover, the functional group on monosaccharides (OH, COO^-) of gellan gum may also form H-bond with NH group of FG (FG-gellan H-bond).

It was noticed that the shifting of amide A from 3432 cm^{-1} in FG to 3418 cm^{-1} in FGe was not statistically significant (Table 4). Nevertheless, this shifting of about 20 cm^{-1} in amide A of FGe still suggest intermolecular interactions between FG and gellan. The current result is consistent to Dong, Wang, and Du (2006) which reported the shifting of amide A from 3421 to 3411 cm^{-1} in alginate-gelatin blended films. In FGe5C & FGe20C, the amide A band down-shifted for more than 100 cm^{-1} and became significantly different from FG (Table 4) ($P < 0.05$) due to H-bond formation between peptide chains of FG. The crosslinking reaction of gellan by Ca^{2+} induced segregative interaction between FG and gellan, hence greater FG-FG association with more H-bonds

Table 4

Characteristic peaks from FTIR spectra. *Within each row, means with different lowercase letters are significantly different ($P < 0.05$) among different groups. *The assignment of the peaks was based on the reports from Barth (2007) and Sow and Yang (2015).

Region	Wavenumber (cm^{-1})					Assignment
	BG	FG	FGe	FGe5C	FGe20C	
Amide A	$3429 \pm 7^{\text{a}}$	$3432 \pm 3^{\text{a}}$	$3418 \pm 10^{\text{a}}$	$3339 \pm 4^{\text{c}}$	$3376 \pm 40^{\text{b}}$	N-H stretch coupled with intramolecular H-bond
Amide B	$3085 \pm 2^{\text{a}}$	$3085 \pm 0^{\text{a}}$	$3085 \pm 1^{\text{a}}$	$3085 \pm 1^{\text{a}}$	$3083 \pm 1^{\text{a}}$	NH bend
Amide I	$1661 \pm 2^{\text{a}}$	$1663 \pm 0^{\text{a}}$	$1662 \pm 3^{\text{a}}$	$1662 \pm 1^{\text{a}}$	$1659 \pm 2^{\text{a}}$	C=O stretch/hydrogen bond coupled with COO^-
Amide II	$1556 \pm 6^{\text{a}}$	$1553 \pm 2^{\text{a}}$	$1554 \pm 2^{\text{a}}$	$1555 \pm 2^{\text{a}}$	$1556 \pm 3^{\text{a}}$	NH bend coupled with CN stretch
Amide III	$1240 \pm 0^{\text{a}}$	$1241 \pm 1^{\text{a}}$	$1241 \pm 2^{\text{a}}$	$1240 \pm 0^{\text{a}}$	$1240 \pm 0^{\text{a}}$	NH bend stretch coupled CN stretch

formation. The large standard deviation ($\pm 40 \text{ cm}^{-1}$) of amide A in FGe20C also supported the high heterogeneity of FGe20C as observed by AFM. The large standard deviation of FGe20C was because part of the spectra collected resembled FGe with the characteristic of FG-gellan complex (shifting in amide A of about 20 cm^{-1}), and part of the spectra retained the property of FGe5C which contained greater FG-FG associated complexed that induced by segregative FG-gellan interaction (shifting in amide A of about 100 cm^{-1}).

Deconvolution of amide I provided detailed secondary structure information of proteins (Barth, 2007), as shown in Fig. 4a. The component peaks could be assigned into various secondary structures by comparing to the literature reports (Barth, 2007; Weng, Zheng, & Su, 2014). Helix structure ($1654\text{--}1662 \text{ cm}^{-1}$), disordered coil ($1642\text{--}1650 \text{ cm}^{-1}$), β -sheet ($1611\text{--}1640 \text{ cm}^{-1}$) and β -turn ($1665\text{--}1693 \text{ cm}^{-1}$) were identified in Fig. 4a. The secondary structures were estimated by the area of the component peaks under amide I band as showed in Fig. 4b. In particular, the area percentage ratio of helix to coil structure (Fig. 4c) can be used to estimate the triple helix content in gelatin, which is highly correlated with the tensile strength of gelatin film (Weng et al., 2014).

Wang and Padua (2012) reported that nanosphere of zein could be originated from α -helix, transformed and aggregated into spherical structure through four step transformation. Interestingly, in the current study, there was an inverse correlation between the helix to coil ratio (Fig. 4c) and the spherical aggregates' diameter (Table 2). As the spherical aggregates diameter of FG was the greatest, the helix to coil ratio of FG was the lowest. While modification of FG decreased the diameter of aggregates, the helix/coil ratio increased upon addition of gellan and CaCl_2 . The spherical aggregates' diameter and helix to coil ratio of FGe20C matched that of BG. The spherical aggregates were assigned as the result of association of gelatin peptide chains in the schematic model. As the high helix to coil ratio also indicated strong re-association of gelatin chains, the inverse correlation between the secondary and nanostructure could be explained. When the association of gelatin chains was stronger, the helix to coil ratio increased and the aggregates became more compact and smaller in diameter. The lower the triple helix content of FG, the less the gel strength (Weng et al., 2014). With this inverse correlation between triple helix content and diameter of spherical aggregates, it further explained why large spherical aggregates led to lower gel strength in FG. The helix to coil ratio could therefore another critical factor determining the texture of gelatin.

4. Conclusions

The mixed biopolymer system consisted of 6.67 g/100 mL 160 Bloom FG, 0.1 g/100 mL gellan and 20 mmol/L CaCl_2 matched the texture, T_m and T_g of 240 Bloom BG. The success of FG modification was allowed by co-existence of the mixture of gellan-FG amorphous structure, segregative region of fibrous gellan aggregates, and spherical FG aggregates, these structures were able to increase

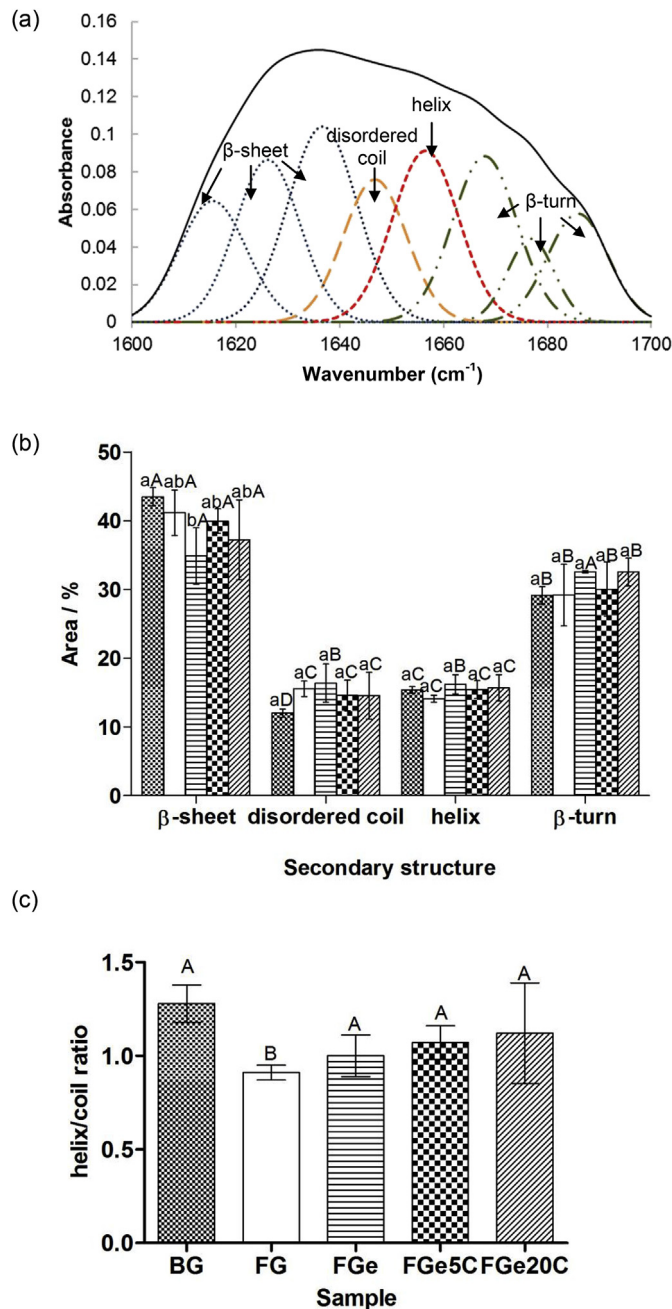
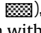
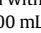

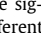
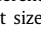


Fig. 4. Deconvoluted amide I band featuring (a) the component and corresponding secondary structures, (b) the content of secondary structures of beef gelatin (BG, ) fish gelatin (FG, ) fish gelatin with 0.1 g/100 mL gellan (FGe, ) fish gelatin with 0.1 g/100 mL gellan and 5 mmol/L CaCl₂ (FGe5C, ) and fish gelatin with 0.1 g/100 mL gellan and 20 mmol/L CaCl₂ (FGe20C, ) as well as (c) the helix to coil ratio.

*Within each secondary structure, groups with different lowercase letters have significant statistical difference ($P < 0.05$). For the same sample, groups with different capital letters have significant statistical difference ($P < 0.05$) among different size ranges.

the rigidity of the FG gel. The diameter of spherical aggregates and the helix to coil ratio were critical nano and secondary structure features, matching of which determined the success of modifying of FG to be BG replacer. Overall, the current results demonstrate that it is feasible to replace mammalian gelatin with FG through adding food grade components into FG, thus meeting the gelatin demand of religious people.

Appendix A. Supplementary data

Supplementary data related to this article can be found at <http://dx.doi.org/10.1016/j.lwt.2017.07.014>.

References

- Ahmad, M., & Benjakul, S. (2011). Characteristics of gelatin from the skin of unicorn leatherjacket (*Aluterus monoceros*) as influenced by acid pretreatment and extraction time. *Food Hydrocolloids*, 25, 381–388.
- Barth, A. (2007). Infrared spectroscopy of proteins. *Biochimica et Biophysica Acta (BBA) - Bioenergetics*, 1767, 1073–1101.
- Boran, G., Mulvaney, S. J., & Regenstein, J. M. (2010). Rheological properties of gelatin from silver carp skin compared to commercially available gelatins from different sources. *Journal of Food Science*, 75, E565–E571.
- Derkach, S. R., Ilyin, S. O., Makiakova, A. A., Kulichikhin, V. G., & Malkin, A. Y. (2015). The rheology of gelatin hydrogels modified by κ -carrageenan. *LWT - Food Science and Technology*, 63, 612–619.
- Dong, Z., Wang, Q., & Du, Y. (2006). Alginate/gelatin blend films and their properties for drug controlled release. *Journal of Membrane Science*, 280, 37–44.
- Feng, X., Bansal, N., & Yang, H. (2016). Fish gelatin combined with chitosan coating inhibits myofibril degradation of golden pomfret (*Trachinotus blochii*) fillet during cold storage. *Food Chemistry*, 200, 283–292.
- Feng, X., Fu, C., & Yang, H. (2017). Gelatin addition improves the nutrient retention, texture and mass transfer of fish balls without altering their nanostructure during boiling. *LWT - Food Science and Technology*, 77, 142–151.
- Feng, X., Ng, V. K., Miks-Krajnik, M., & Yang, H. (2017). Effects of fish gelatin and tea polyphenol coating on the spoilage and degradation of myofibril in fish fillet during cold storage. *Food and Bioprocess Technology*, 10, 89–102.
- Fonkwe, L. G., Narsimhan, G., & Cha, A. S. (2003). Characterization of gelation time and texture of gelatin and gelatin–polysaccharide mixed gels. *Food Hydrocolloids*, 17, 871–883.
- Funami, T., Noda, S., Nakauma, M., Ishihara, S., Takahashi, R., Al-Assaf, S., et al. (2008). Molecular structures of gellan gum imaged with atomic force microscopy (AFM) in relation to the rheological behavior in aqueous systems in the presence of sodium chloride. *Food Hydrocolloids*, 23, 548–554.
- Hans Tromp, R., van de Velde, F., van Riel, J., & Paques, M. (2001). Confocal scanning light microscopy (CSLM) on mixtures of gelatine and polysaccharides. *Food Research International*, 34, 931–938.
- Kaewruang, P., Benjakul, S., Prodpran, T., Encarnacion, A. B., & Nalinanon, S. (2014). Impact of divalent salts and bovine gelatin on gel properties of phosphorylated gelatin from the skin of unicorn leatherjacket. *LWT - Food Science and Technology*, 55, 477–482.
- Lau, M. H., Tang, J., & Paulson, A. T. (2000). Texture profile and turbidity of gellan/gelatin mixed gels. *Food Research International*, 33, 665–671.
- Lau, M. H., Tang, J., & Paulson, A. T. (2001). Effect of polymer ratio and calcium concentration on gelation properties of gellan/gelatin mixed gels. *Food Research International*, 34, 879–886.
- Lee, K. Y., Shim, J., Bae, I. Y., Cha, J., Park, C. S., & Lee, H. G. (2003). Characterization of gellan/gelatin mixed solutions and gels. *LWT - Food Science and Technology*, 36, 795–802.
- Liu, S., & Wang, Y. (2011). Chapter 6—a review of the application of atomic force microscopy (AFM) in food science and technology. In L. T. Steve (Ed.), *Advances in food and nutrition research* (Vol. 62, pp. 201–240). Academic Press.
- Mohtar, N. F., Perera, C., & Quek, S.-Y. (2010). Optimisation of gelatine extraction from hoki (*Macruronus novaezelandiae*) skins and measurement of gel strength and SDS–PAGE. *Food Chemistry*, 122, 307–313.
- Morris, E. R., Nishinari, K., & Rinaudo, M. (2012). Gelation of gellan — a review. *Food Hydrocolloids*, 28, 373–411.
- Myshakina, N. S., Ahmed, Z., & Asher, S. A. (2008). Dependence of amide vibrations on hydrogen bonding. *The Journal of Physical Chemistry B*, 112, 11873–11877.
- Nieto Nieto, T. V., Wang, Y., Ozimek, L., & Chen, L. (2016). Improved thermal gelation of oat protein with the formation of controlled phase-separated networks using dextrin and carrageenan polysaccharides. *Food Research International*, 82, 95–103.
- Pang, Z., Deeth, H., Sopade, P., Sharma, R., & Bansal, N. (2014). Rheology, texture and microstructure of gelatin gels with and without milk proteins. *Food Hydrocolloids*, 35, 484–493.
- Panouillé, M., & Larreta-Garde, V. (2009). Gelation behaviour of gelatin and alginate mixtures. *Food Hydrocolloids*, 23, 1074–1080.
- Pew Research Center. (2014). *Global religious diversity: Half of the most religiously diverse countries are in Asia-Pacific region*. <http://www.pewforum.org/files/2014/04/Religious-Diversity-full-report.pdf> (Accessed 18 October 2015).
- Pranoto, Y., Lee, C. M., & Park, H. J. (2007). Characterizations of fish gelatin films added with gellan and κ -carrageenan. *LWT - Food Science and Technology*, 40, 766–774.
- Razzak, M. A., Kim, M., & Chung, D. (2016). Elucidation of aqueous interactions between fish gelatin and sodium alginate. *Carbohydrate Polymers*, 148, 181–188.
- Saxena, A., Sachin, K., Bohidar, H. B., & Verma, A. K. (2005). Effect of molecular weight heterogeneity on drug encapsulation efficiency of gelatin nano-particles. *Colloids and Surfaces B: Biointerfaces*, 45, 42–48.
- Singh, P., Benjakul, S., Maqsood, S., & Kishimura, H. (2011). Isolation and characterisation of collagen extracted from the skin of striped catfish (*Pangasianodon*

- hypophthalmus*). *Food Chemistry*, 124, 97–105.
- Sow, L. C., & Yang, H. (2015). Effects of salt and sugar addition on the physico-chemical properties and nanostructure of fish gelatin. *Food Hydrocolloids*, 45, 72–82.
- Wang, Y., & Padua, G. W. (2012). Nanoscale characterization of zein self-assembly. *Langmuir*, 28, 2429–2435.
- Weng, W., Zheng, H., & Su, W. (2014). Characterization of edible films based on tilapia (*Tilapia zillii*) scale gelatin with different extraction pH. *Food Hydrocolloids*, 41, 19–26.
- Yang, H., & Wang, Y. (2009). Effects of concentration on nanostructural images and physical properties of gelatin from channel catfish skins. *Food Hydrocolloids*, 23, 577–584.
- Yasin, H., Babji, A. S., & Ismail, H. (2016). Optimization and rheological properties of chicken ball as affected by κ -carrageenan, fish gelatin and chicken meat. *LWT - Food Science and Technology*, 66, 79–85.